



**Chemical  
Insights**

An Institute of  
Underwriters Laboratories Inc.

SUMMARY OF PROGRESS REPORT 1

# Physicochemical and Toxicological Characterization of Electronic Nicotine Delivery Systems

Provided by Georgia State University, School of Public Health

SEPTEMBER 2021

## TABLE OF CONTENTS

1.	INTRODUCTION	3
2.	EXPERIMENTAL METHODS	3
3.	RESULTS AND DISCUSSION	5
4.	CONCLUSIONS	9
5.	CHALLENGES	10
6.	REFERENCES	10

## TABLE OF FIGURES

<b>Figure 1:</b>	Induction of reactive oxygen species by pod flavored aerosols after 24 hours and 7 days at two device age states (puffs 1-50 and 101-150).	7
<b>Figure 2:</b>	Oxidative stress induced by ENDS aerosol exposures for pods (A,B) and tanks with flavored e-liquid (C,D). Significant reduction in cellular glutathione levels was observed at both 24 hours and 7 days, indicating oxidative stress and the presence of reactive oxygen species. C. After 24 hours, tank exposures did not modulate SAEC viability; however, after 7 days, a significant reduction in total glutathione levels was observed indicating repeated exposures contribute to oxidative stress.	8
<b>Figure 3:</b>	Cellular viability of SAEC exposed to ENDS aerosol exposures for pods (A,B) and tanks with flavored e-liquid (C,D). At 24 hours post-exposure, no significant change in cellular viability was observed in SAEC. However, at 7 days, a 25% reduction in metabolic capacity, an indicator of cellular viability, was found in both device age states for pods. Tank aerosols after 7 days revealed a significant reduction in the puffs 1-25 age state.	8
<b>Figure 4:</b>	Single stranded DNA damage observed following exposure to pods aerosols after 24 hours and 7 days of repeated exposures.	9

## 1. INTRODUCTION

The overarching goal of this study is to examine the physicochemical and toxicological properties of particulate and volatile emissions from electronic nicotine delivery systems (ENDS). Given that ENDS use has increased dramatically in the United States in the last decade, particularly amongst adolescents and young adults, it is imperative the scientific community investigate the public health effects of exposure to these products. To accomplish this aim, we collected samples from two of the most popular ENDS products on the market: a pod-type device and a tank device (i.e., contains a refillable reservoir for the vaping liquid). This report describes the sample collection and toxicological assessment methodology, preliminary findings, limitations and challenges encountered, and future directions. A description of the research initiative and academic partners are presented here [https://chemicalinsights.org/wp-content/uploads/2019/11/ENDS\\_Technical-Brief.pdf](https://chemicalinsights.org/wp-content/uploads/2019/11/ENDS_Technical-Brief.pdf).

## 2. EXPERIMENTAL METHODS

**Puff generation.** We used a custom-built 4-channel robotic “puff generator”. The puff flow from each device was directed to a 1L buffer chamber located underneath of ENDS devices. The buffer chamber was diluted with clean air at a user-determined flow rate between 0-10 LPM, and the outflow from the buffer chamber exits through a 7-port manifold. The puff generator was placed inside a 6 m<sup>3</sup> exposure chamber at the Chemical Insights’ Toxicology Center with a chamber air exchange rate of three changes per hour. ENDS were automatically activated at the start of each puff using a pneumatic actuator. We used a realistic puff topography consisting of a 50 ml volume and 3.5 seconds duration. During initial experiments, we used an inter-puff interval of 30 seconds based on the Center for Scientific Research Relative to Tobacco (CORESTA) recommended method; however, we subsequently modified the inter-puff interval to 192 seconds to more closely match real-world use as well as to allow sufficient time for the chamber to reach equilibrium for collection of volatile emissions. Although the puff generator is capable of simultaneously operating four devices, for experiments with pod devices, we initially used three devices simultaneously. However, after observing that one device was sufficient to collect a suitable sample volume, we subsequently used one device at a time. For tank devices, we used one device at a time in all experiments.

**Device aging.** For both pod and tank devices, we designed the experiments to collect a sample at the new, broken-in, and aged state. For pod devices, the “new” state corresponded to puffs 1-50, and “broken-in” was set as puffs 101-150; however, in practice, pods rarely lasted much longer than 150 puffs, and therefore, only two age states were used for these devices. For tank devices, the “new” state corresponded to puffs 1-25, “broken-in” was set as puffs 101-125, and “aged” was established as puffs 201-225. After examining online user reviews and social media posts related to tank devices of this and similar brands, we determined the “coils” (the replaceable component containing the heating element and wick) are rarely used longer than this by most users.

**ENDS and e-liquid selection.** All ENDS devices and liquids were purchased in-person from local vaping shops. For both pod and tank devices, we selected the most neutral flavor available. For pod devices, we selected the 3% nicotine pod (the lower of the two concentrations). For the tanks, we selected a tobacco-flavored e-liquid at a nicotine strength of 3 mg/ml, which is a similar nicotine level as the 3% pods.

**Electronic control settings.** For pod devices, we operated the puff generator at a constant voltage of 3.7V, which is the nominal voltage for the batteries. For the coils used in the tanks, they are marketed according to the resistance of the coil with a lower resistance corresponding to a higher wattage, and thus a higher temperature and a larger vape plume. Each coil has a recommended wattage range, and we collected samples from each end of the range. Due to internal electrical resistance, the voltage setting entered into the puff generator controls differed from that delivered to the ENDS device. For pod devices, the power supply voltage matched the voltage delivered by a charged pod battery. For tank devices, we used trial and error to determine the power supply voltage that would produce the desired wattage as measured at the coil. Table 1 shows the electronic control settings for all experimental set-ups.

Device	Coil Resistance [ $\Omega$ ]	Power Supply Voltage [ V ]	ENDS Wattage [ W ]
Pod	not specified	3.7	6.6
Tank	0.2	3.0	40
Tank	0.2	3.5	60
Tank	0.6	3.5	20
Tank	0.6	5.6	28

**Sample collection.** We collected ENDS emissions using fluorinated ethylene propylene (FEP) tube condensation traps. All FEP tubes were pre-cleaned using a solution of nitric and hydrochloric acid followed by rinses with methanol and ultrapure water. The tubes have an inner diameter of 3.97 mm such that a 404 cm length of tubing corresponds to the volume of one puff (50 ml). The first

successful experiment used one FEP tube line connected to the buffer chamber exhaust manifold, while all subsequent experiments used two FEP tube lines; however, the exact length of tubing varied by experiment. A third port on the exhaust manifold vented to the exposure chamber, and the remaining four ports were capped. The FEP tubing was followed by an after-filter composed of either a polytetrafluoroethylene (PTFE) membrane, polycarbonate (PC) membrane, or glass fiber (GF) matrix. The flow rate through each sample tube was set at 1 LPM. While the buffer chamber dilution flow varied by experiment, it exceeded the sample flow for all experiments such that some flow from the buffer chamber was vented into the exposure chamber. All tubes, filters, and e-liquid pods or tanks were weighed before and after the experiment to determine by gravimetric difference the mass vaporized and collected. The set-up parameters for all successfully completed experiments are shown in Table 2.

Start Date	Device and Coil	Number of Devices	ENDS Wattage [ W ]	Dilution Flow [ LPM ]	FEP Tube Length [ cm ]	Filter Material
8/21/20	POD	3	6.6	1.0	914	PC
8/26/20	POD	3	6.6	2.3	1822	-
9/2/20	POD	3	6.6	2.0	1822	GF
9/9/20	POD	3	6.6	2.1	1826	PC
10/2/20	POD	1	6.6	2.1	1822	PC
1/25/21	Tank, 0.2Ω	1	40	2.1	2748	GF
2/3/21	Tank, 0.6Ω	1	20	2.1	2748	GF
2/10/21	Tank, 0.2Ω	1	60	3.0	2460	GF
2/17/21	Tank, 0.6Ω	1	28	3.0	2752	GF

**Sample extraction.** ENDS emissions that deposited or condensed in the FEP condensation tubes were extracted by filling them with 75% methanol, capping the ends, and sonicating for five minutes at 25° C. We then aspirated the liquid from the tubing, vacufuged down to 0.5 ml, and stored the sample at 4° C until toxicological testing.

**Dosimetry for cellular assays.** We used the Multiple Path Particle Dosimetry (MPPD) model for particle dosimetry. The MPPD is a stochastic lung model used to estimate deposition in small airways following oral-pharyngeal exposure based on aerosol number concentration and geometric mean diameter. The model outputs are deposited mass (µg) per deposited surface area (cm<sup>2</sup>), from which we determined the deposited dose (µg/cm<sup>2</sup>). To convert the total deposited dose to an in vitro concentration, we multiplied the total deposited dose by the surface area of one well within a 24-well trans-well plate (0.33 cm<sup>2</sup>) then multiplied by the total exposure volume (0.1 ml).

**Cell culture and ENDS exposure procedures.** We used human Small Airway Epithelial Cells (SAEC) for all cellular toxicological assays. SAEC were expanded for a period of 3-4 days until reaching 70-80% confluency. Upon confluency, we seeded SAEC into trans-well inserts contained in 24-well plates and maintained with a complete growth medium. We changed the growth media every two days for a period of 10 days. After a complete monolayer was achieved, SAEC were air-lifted by aspirating media off the apical surface of the cell monolayer, while the basolateral media was changed every 2-3 days until day of exposure. ENDS sample extracts were administered directly to the apical side of SAEC grown within trans-well inserts daily for 7 days or once for a 24-hour exposure.

**Oxidative stress.** We used the GSH-Glo™ luminescent assay for the detection and quantification of glutathione (GSH) in cells or in various biological samples. A change in GSH levels is an indicator of oxidative stress and can potentially lead to apoptosis or cell death over time. ENDS exposed SAEC were probed for total glutathione levels after 24 hours and seven days of exposure. After exposure, we washed the cells with phosphate buffered saline (PBS) and measured luminescence using a Cytation 1 spectrophotometer.

**Cellular viability measurements.** Metabolic activity was assessed by measuring the amount of a tetrazolium salt compound (MTS) that is biologically reduced by metabolically active cells. Following the cell exposure protocol, exposed cells were washed with PBS, and fresh media containing the MTS reagent was added to the apical compartment/cells and incubated for one hour. Plates were read at 490 nm using a Cytation 1 spectrophotometer.

**DNA damage detection.** Increased levels of reactive oxygen species (ROS) can induce DNA single strand breaks, double strand breaks, and reduce DNA repair efficiency. We used the CometChip® high-throughput assay to evaluate ENDS-mediated DNA damage in SAEC. This system uses a 96-well gel embedded with thousands of individual mini-wells (40 µm in diameter) into which single cells deposit by gravitational settling. We harvested ENDS exposed SAEC from trans-well inserts and dispersed them into the individual macrowells of the CometChip®. The individual cells were embedded in a top agarose gel layer then lysed using an alkaline lysis solution followed by 30 minutes of electrophoresis and subsequent staining with SYBR Gold nucleic acid stain.

**CometChip® imaging and scoring.** Multiple images of the CometChip® gel were taken using the Cytation 1 Imaging System. Damaged cells or nuclei resemble a comet with a distinct head and tail. The head is composed of intact DNA, while the tail consists of damaged (single-strand or double-strand breaks) or broken fragments of DNA. The length and intensity of the comet tail are indicators of the level of DNA damage. We used Image J (NIH) software coupled with OpenComet ([cometbio.org](http://cometbio.org)) analysis to score a total of 100 comets per exposure group and controls.

**Statistical analysis.** All experimental groups were completed in triplicate and individual experimental trials were completed in duplicate. We performed one-way ANOVA statistical analysis using GraphPad Prism software with significance established a priori at  $\alpha \leq 0.05$ .

### 3. RESULTS AND DISCUSSION

**ENDS aerosol concentration.** We used a TSI, Inc. scanning mobility particle sizer (SMPS) and optical particle sizer (OPS) to measure the aerosol concentration and size distribution inside the exposure chamber. The concentration inside the chamber depends on numerous experimental parameters, including the ratio of sample flow to dilution flow, the number of devices in use, the inter-puff interval, and the coil resistance and wattage. The average aerosol mass concentration and geometric mean diameter (GMD) for each ENDS device and e-liquid are shown in Table 3. Since three devices were used simultaneously for most pod experiments, the average particle concentration for POD experiments was substantially higher than for Tank experiments. The average GMD was also larger for pods, reflecting more particle coagulation and differences in e-liquid formulation.

Device	Device Age	Mass concentration [ $\mu\text{g}/\text{m}^3$ ]	GMD [ $\mu\text{m}$ ]
POD	puffs 1-50	208	1.19
POD	puffs 101-150	153	1.29
Tank	puffs 1-25	7.6	0.156
Tank	puffs 101-25	1.7	0.133
Tank	puffs 201-225	4.7	0.0931

**ENDS mass emissions and sample collection.** For each experiment, we gravimetrically measured the mass of e-liquid vaporized and the mass that was collected in the condensation tubes and on the filters. In addition, we frequently observed e-liquid vapor condensed inside of the buffer chamber. This data is shown in Table 4. We can make a number of initial observations from this preliminary data.

- First, in a few cases, the total mass collected in the condensation tubes, after-filters, and buffer chamber exceeded the mass vaporized. A likely explanation for this finding is that the excess mass is due to condensation of water vapor present in exposure chamber air.
- Second, low resistance coils vaporize more e-liquid than high resistance coils, and furthermore, each coil vaporizes a larger mass when used at higher power settings. This is because higher wattage directly results in higher coil temperature, which results in more e-liquid vaporization. The highest temperature experiment, the 0.2 $\Omega$  coil operated at 60W, vaporized almost four times as much e-liquid as the lowest temperature experiment, the 0.6 $\Omega$  coil operated at 20W.
- Third, more mass was collected in the condensation tubes from low-temperature experiments even though these experiments vaporized less e-liquid. The reasons for this observation are less clear, but may be related to the formation of larger particles which preferentially deposit on the interior surfaces of the condensation tubes.

Start Date	Device, Coil, and Wattage	Device Age	Mass Vaporized [ mg ]	Mass Collected [ mg ]	Percent Collected	Mass in Buffer Chamber [ mg ]
8/21/20	Pod 6.6 W	1-150	1285	81.0	6.3%	not measured
8/26/20	Pod 6.6 W	1-150	1250	159	13%	10
9/2/20	Pod 6.6 W	1-150	1305	114	8.7%	not measured
9/9/20	Pod 6.6 W	1-50	1032	124	12%	not measured
		101-150	1025	219	21%	not measured
10/2/20	Pod 6.6 W	1-50	170	46.0	27%	not measured
		101-150	78.0	51.0	65%	not measured
1/25/21	Tank 0.2Ω, 40 W	1-25	1558	1065	68%	1140
		101-125	1647	1170	71%	1295
		201-225	1550	636	41%	85
2/3/21	Tank 0.6Ω, 20 W	1-25	1302	997	77%	358
		101-125	706	1094	155%	265
		201-225	756	713	94%	130
2/10/21	Tank 0.2Ω, 60 W	1-25	2648	225	8.5%	1968
		101-125	2716	633	23%	2040
		201-225	2562	554	22%	1610
2/17/21	Tank 0.6Ω, 28 W	1-25	1230	265	22%	550
		101-125	1240	930	75%	655
		201-225	1254	820	65%	640

- Fourth, the pods produce noticeably fewer emissions than the tanks. Some of this reduction may be related to differences in e-liquid formulation; however, we suspect a more important explanation is the lower temperature of the pod coils. Although the resistance of the pod coils is not specified, we can use Ohm's Law to calculate the resistance from the measured power and voltage and find it is approximately 2Ω. This comparatively high resistance and low wattage would suggest a relatively low coil temperature for pod experiments when compared to the tank experiments.
- Fifth, we observed substantial variability between experiments even when applying similar experimental parameters. For example, for a small number of experiments, we observed a factor of two difference in either the amount of e-liquid that was vaporized or collected. Potential sources of this variability are leaks in the ENDS devices and reductions in the flow rate through the sample tubes. Device leaks would produce the appearance of more liquid being vaporized, and reduced flow through the condensation tubes would lower the mass collected. We spot-checked sample tube flows repeatedly, but this data could not be continuously logged. We did observe reductions in flow that resulted from loading on the after-filters, which was the primary reason we switched from polycarbonate to glass fiber filters.

**Determination of applied doses.** The ENDS mass collected in the condensation tubes for all experiments is shown in Table 4. Toxicological evaluation of these samples is ongoing; however, we have conducted toxicological assays for two complete experiments: the pod experiment conducted on 10/2/2020 using the flavor with 3% nicotine content and the tank experiment conducted the week of 1/25/2021 using a 0.2Ω coil operated at 40W with tobacco-flavored e-liquid with 3 mg/ml nicotine content. Both experiments included multiple age states: puffs 1-50 and 101-150 for the pod and puffs 1-25, 101-125, and 201-225 for the tank. We used the particle concentration and size distribution measured in the exposure chamber for these experiments as inputs for the MPPD model to estimate the deposited mass of aerosols in the small airways of a human exposed to these aerosols. We have shown the results of these model calculations in Table 5. Please note that since these calculations are based on the exposure chamber aerosol concentration, which is itself dependent on experimental parameters including sample flow rate and buffer chamber dilution flow rate. The in vitro concentration therefore reflects experimental conditions on that particular sample day and not necessarily lung deposition in a human actively using these ENDS devices.

TABLE 5. MPPD MODEL ESTIMATES OF PARTICLE DEPOSITION IN THE SMALL AIRWAYS OF EXPOSED HUMAN LUNGS					
Device and Coil	Device Age State	Average Total Deposited Mass [ μg ]	Average Deposited Surface Area [ cm <sup>2</sup> ]	Average Deposited Dose [ μg/cm <sup>2</sup> ]	in vitro concentration [ μg/ml ]
Pod	puffs 1-50	2.33E-03	1.17E-04	19.9	65.6
Pod	puffs 101-150	1.85E-03	8.61E-05	21.5	71.0
Tank, 0.2Ω	puffs 1-25	9.54E-05	3.66E-05	2.60	8.58
Tank, 0.2Ω	puffs 101-125	2.39E-05	1.07E-05	2.23	7.34
Tank, 0.2Ω	puffs 201-225	8.83E-05	5.69E-05	1.55	5.12

**Reactive Oxygen Species Generation in ENDS exposed SAEC.** Intracellular reactive oxygen species within ENDS exposed SAEC were detected using the CellROX assay. The CellROX dye is cell permeable and is non-fluorescent in its native state. Upon cellular uptake, the stain becomes oxidized and fluorescent orange due to oxidation from ROS present within the cell after ENDS exposure. The nuclei of the cells are stained with blue counterstain. Figure 1 shows qualitative data for reactive oxygen species (ROS) detected in SAEC exposed to flavored pod ENDS aerosols after 24 hours and 7 days. After 24 hours, these exposures elicited significant levels of ROS (Figure 1C and 1D) in comparison to the negative control (Figure 1A) at both device age states of puffs 1-50 and 101-150. After 7 days of repeated exposure to pod aerosols, each device age state showed elevated ROS levels (Figure 1G and 1H) in SAEC relative to the negative control (Figure 1E). Due to pandemic-related delays in receiving necessary supplies, the ROS assessments for tanks with flavored e-liquid are still underway.

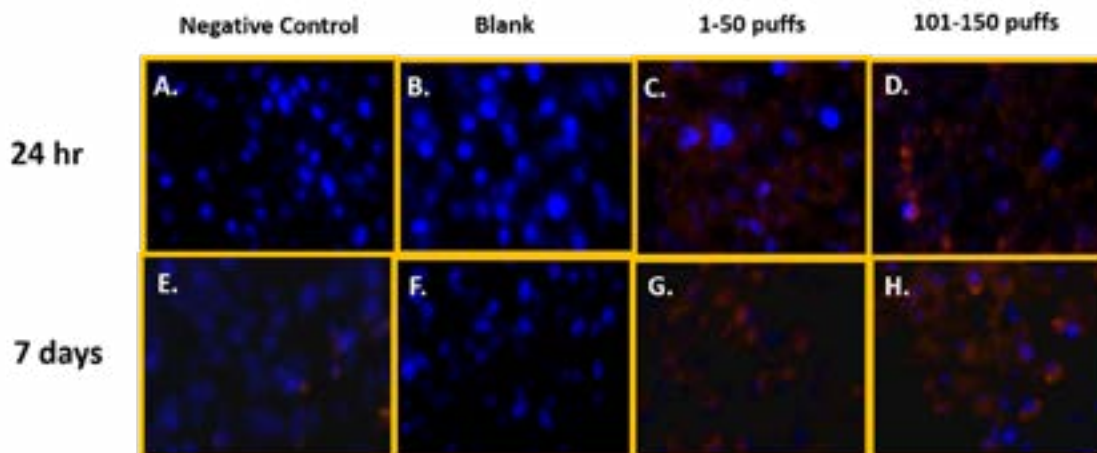


**Figure 1.** Induction of reactive oxygen species by pod flavored aerosols after 24 hours and 7 days at two device age states (puffs 1-50 and 101-150).

**ENDS Aerosols Elicit Oxidative Stress.** Total cellular glutathione is an antioxidant present in all mammalian cells and serves as a biomarker of oxidative stress. Reductions in cellular glutathione have been noted in several airway pathologies including asthma (Fitzpatrick et al 2012) and chronic obstructive pulmonary disease (COPD) (Rahman et al 1999). Decrements in lung glutathione levels are known to be involved in key events that initiate airway remodeling and structural changes that lead to reduced lung function (Yoshida et al 2000). Significant reduction in cellular glutathione was observed after 24-hour exposures to pod aerosols for both 65.6  $\mu\text{g}/\text{ml}$  (1-50 puffs) and 71  $\mu\text{g}/\text{ml}$  (101-150 puffs) (Figure 2A). Likewise, after 7 days of repeated pod exposures, significant reductions in cellular glutathione levels (44% and 40%) were observed indicating oxidative stress (Figure 2B). Tanks with flavored e-liquid aerosols did not elicit a reduction in glutathione levels at 24 hours; however, a prominent reduction in glutathione was observed after 7 days of repeated exposures.

### Total Glutathione

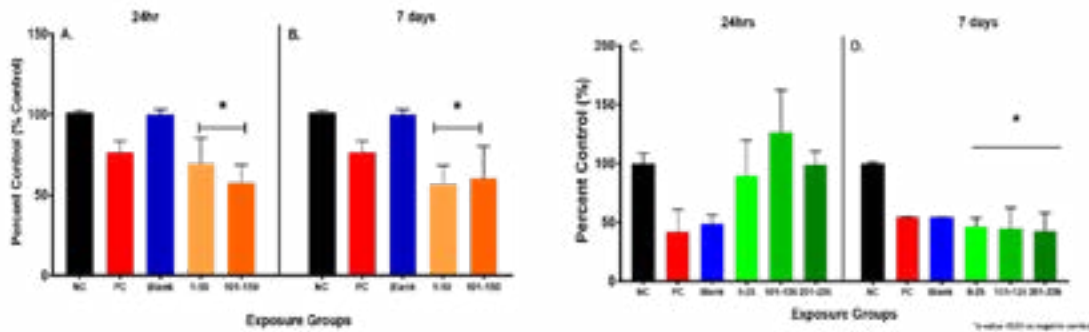


**Figure 2.** Oxidative stress induced by ENDS aerosol exposures for pods (A,B) and tanks with flavored e-liquid (C,D). Significant reduction in cellular glutathione levels was observed at both 24 hours and 7 days, indicating oxidative stress and the presence of reactive oxygen species. C. After 24 hours, tank exposures did not modulate SAEC viability; however, after 7 days, a significant reduction in total glutathione levels was observed indicating repeated exposures contribute to oxidative stress.

### Cellular Viability

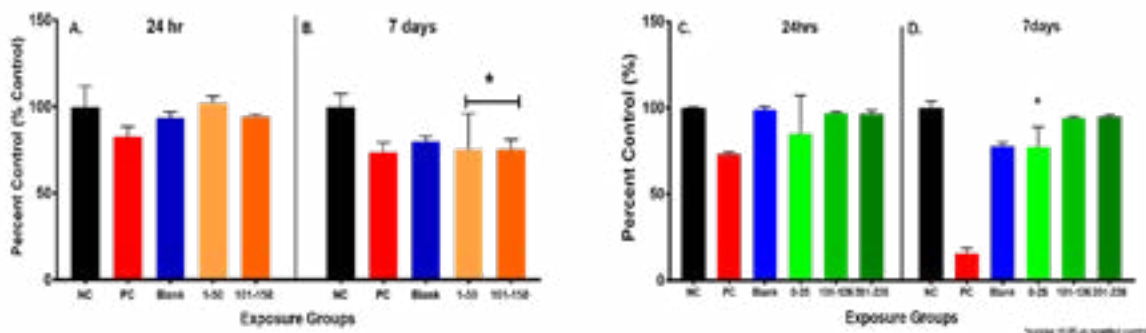


**Figure 3.** Cellular viability of SAEC exposed to ENDS aerosol exposures for pods (A,B) and tanks with flavored e-liquid (C,D). At 24 hours post-exposure, no significant change in cellular viability was observed in SAEC. However, at 7 days, a 25% reduction in metabolic capacity, an indicator of cellular viability, was found in both device age states for pods. Tank aerosols after 7 days revealed a significant reduction in the puffs 1-25 age state.

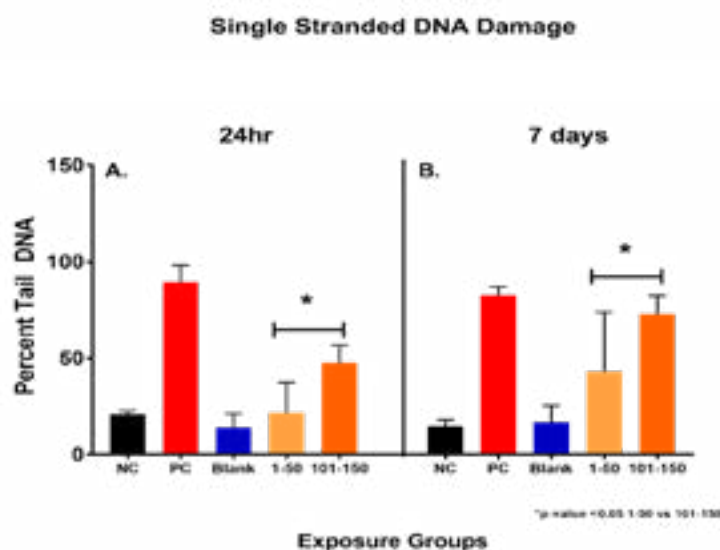


**Figure 4.** Single stranded DNA damage observed following exposure to pods aerosols after 24 hours and 7 days of repeated exposures.

**Impact of pod aerosols on SAEC viability.** We used the MTS assay to evaluate the impact of toxicants on cellular viability. This colorimetric assay uses a cell permeable tetrazolium salt that is metabolically converted by healthy cells into a detectable product called formazan. This process is accompanied by a color shift in the cell culture media/wells from yellow to brownish red. A yellow color indicates unhealthy or damaged cells whereas a reddish color indicates healthy or minimally damaged cells. This reddish product absorbs at the specific wavelength of 490 nm, which can then be converted into an optical density value. The data are normalized by dividing experimental (ENDS exposed) mean optical density values by the mean media control optical density value, which provides the percent control.

**Induction of DNA damage by ENDS Aerosols Exposures in SAEC.** To determine the genotoxicity of ENDS aerosols, we employed the CometChip assay. This is a high-throughput version of the comet assay, which is a widely used technique to determine DNA damage in single cells elicited by oxidative stress. The percent Tail DNA, a metric determined by CometChip assessment and used to quantify the level of DNA damage is shown in Figure 4 for each pod exposure group. We observed a significant increase in single stranded DNA damage at 24 hours for both concentrations and device age states. Longer exposure durations increased single stranded DNA damage levels above the 24-hour levels and potentially contributed to the reduction in cellular viability observed in Figure 1. Due to pandemic-related delays in receiving necessary supplies, the DNA damage assessments for tanks with flavored e-liquid are still underway.

## 4. CONCLUSIONS

Our preliminary aerosol and toxicological analyses indicate there are noteworthy differences between the pod and tank ENDS evaluated in this study. Aerosol concentrations varied significantly between the ENDS devices. These differences are related to some extent to e-liquid formulations, but importantly, also to factors that influence the coil temperature including the coil resistance and the amount of power applied. In addition, the concentration of aerosols inside the exposure chamber is strongly influenced by experimental parameters, including the inter-puff interval, the dilution flow rate through the buffer chamber, and the sample flow rate through the condensation tubes. Ongoing toxicological assessment demonstrates clear toxicity of both types of ENDS devices and e-liquids using multiple methods of evaluation.

## 5. CHALLENGES

We encountered several challenges related to logistics, equipment, and methodology.

- First and foremost, the planned start of sample collection for this project unfortunately coincided with the COVID-19 pandemic. This resulted in a 5-month delay in any sampling activities followed by reductions in staffing and an extended schedule once sampling did resume. In addition, many of the reagents and other supplies required for our toxicological assessment are also used in COVID-19 testing and research, and therefore many of these supplies are simply unavailable for non-COVID work or are backordered for several months or more. This includes the culture vessels (air-liquid trans-wells) we use to grow SAEC and expose them to ENDS aerosols. Without these key laboratory supplies, toxicological evaluation cannot proceed. In some cases, we have identified and ordered similar supplies from different brands or models; however, even in these cases, the alternatives also have supply chain issues that impact study progress.
- Second, the puff generator was newly designed and custom-built for this project, and therefore did not have the benefit of reflecting numerous iterations of testing and evaluation. An important design factor that set back our sample collection for weeks is the horizontal configuration of the ports for holding multiple ENDS devices during sampling. This horizontal geometry leads to the wicks in tank experiments becoming dry if they are not completely immersed in e-liquid (this does not affect pod devices since their smaller size allows capillary action to maintain a wetted wick). We discovered that in practice, wick drying occurs after only moderate use and results in the coil becoming hot enough to combust the wick material. This would be unlikely to occur in real-life use since the device would typically be placed in the vertical direction after each puff. In addition, a human user would be able to notice by smell or taste that the coil was overheating. We were able to overcome this challenge by tilting the entire puff generator on its side, but this problem resulted in several burned coils in a row and cost several weeks of study time. In addition, this work-around limits the puff generator to only two devices in use simultaneously.
- Third, we discovered that in practice, polycarbonate filters become saturated with condensed e-liquid after only a few puffs, at which point the pores are blocked and sample flow quickly decreases. We chose polycarbonate substrates due to their suitability for both gravimetric and SEM analysis. SEM analysis was discovered to not be informative because the membrane surfaces were completely covered with condensed e-liquid, which hampered identification of deposited solid-phase particles. In all cases of SEM analysis of polycarbonate filters, only one or two solid particles were identified, and their elemental composition was consistent with wick material or extraneous room dust and inconsistent with material shed from the heating element. Given the problems with maintaining sample flow and the lack of useful information from SEM analysis, we switched to low-pressure drop glass fiber filters that are appropriate for gravimetric analysis.
- Fourth, we learned there is a surprising amount of volatility in the consumer market for ENDS products. Even within the compressed timeline of this study, we discovered products we had begun to evaluate had been discontinued and were no longer available for sale, other products had been upgraded so our purchased models were obsolete, and device parameters we had proposed to investigate were no longer relevant in terms of market share and prevalence amongst ENDS users.
- Fifth, we encountered other minor methodological and equipment challenges. For example, we discovered excessive condensation in the buffer chamber. The amount of condensation is related to longer residence time in the buffer chamber. Residence time can be decreased by increasing the dilution flow, but this decreases the proportion of sample that flows through the condensation tubes and increases the amount that vents to the exposure chamber. We are still evaluating, through trial and error, the optimal balance of dilution flow to sample flow that permits both condensation tube sample collection and volatile emissions analysis from exposure chamber air. In addition, we modified our protocol for gravimetric analysis of condensation tubes. We purchased a balance with 1 mg sensitivity and 200 g capacity and perform all tube weight measurements in a vibration-protected weighing chamber in our laboratory at GSU.

## 6. REFERENCES

Fitzpatrick, A. M., Jones, D. P., & Brown, L. A. Glutathione redox control of asthma: from molecular mechanisms to therapeutic opportunities. *Antioxidants & Redox Signaling* 2012 17(2), 375–408. <https://doi.org/10.1089/ars.2011.4198>

Irfan Rahman and William MacNee. [Lung glutathione and oxidative stress: implications in cigarette smoke-induced airway disease.](#) *American Journal of Physiology-Lung Cellular and Molecular Physiology* 1999 277:6, L1067-L1088.

Toshinori Yoshida and Rubin M. Tuder. [Pathobiology of Cigarette Smoke-Induced Chronic Obstructive Pulmonary Disease.](#) *Physiological Reviews* 2007 87:3, 1047-1082

Li, Y., Fairman, R. T., Churchill, V., Ashley, D. L., & Popova, L. Users' Modifications to Electronic Nicotine Delivery Systems (ENDS): Interviews with ENDS Enthusiasts. *International Journal of Environmental Research and Public Health* 2020 17(3), 918. <https://doi.org/10.3390/ijerph17030918>



An Institute of Underwriters Laboratories Inc.  
2211 Newmarket Parkway, Suite 106, Marietta, GA 30067  
[chemicalinsights@ul.org](mailto:chemicalinsights@ul.org)  
[chemicalinsights.org](http://chemicalinsights.org)